Hindawi Publishing Corporation
EURASIP Journal on Advances in Signal Processing
Volume 2008, Article ID 513873, 11 pages
doi:10.1155/2008/513873

Research Article

The Effect of Cooperation on Localization Systems Using UWB Experimental Data

Davide Dardari,[1] Andrea Conti,[2] Jaime Lien,[3] and Moe Z. Win[4]

[1] *WiLAB, University of Bologna, Viale Risorgimento 2, 40136 Bologna, Italy*
[2] *ENDIF and WiLAB, University of Ferrara, Via Saragat 1, 44100 Ferrara, Italy*
[3] *Jet Propulsion Laboratory, 4800 Oak Grove Drive, Pasadena, CA 91109, USA*
[4] *Laboratory for Information and Decision Systems (LIDS), Massachusetts Institute of Technology, 77 Massachusetts Avenue, Cambridge, MA 02139, USA*

Correspondence should be addressed to Andrea Conti, a.conti@ieee.org

Received 1 September 2007; Accepted 21 December 2007

Recommended by Erchin Serpedin

Localization systems based on ultrawide bandwidth (UWB) technology have been recently considered for indoor environments, due to the property of UWB signals to resolve multipath and penetrate obstacles. However, line-of-sight (LoS) blockage and excess propagation delay affect ranging measurements thus drastically reducing the localization accuracy. In this paper, we first characterize and derive models for the range estimation error and the excess delay based on measured data from real ranging devices. These models are used in various multilateration algorithms to determine the position of the target. Using measurements in a real indoor scenario, we investigate how the localization accuracy is affected by the number of beacons and by the availability of priori information about the environment and network geometry. We also examine the case where multiple targets cooperate by measuring ranges not only from the beacons but also from each other. An iterative multilateration algorithm that incorporates information gathered through cooperation is then proposed with the purpose of improving the localization accuracy. Using numerical results, we demonstrate the impact of cooperation on the localization accuracy.

1. INTRODUCTION

The need for accurate and robust localization (also known as positioning and geolocation) has intensified in recent years. A wide variety of applications depend on position knowledge, including the tracking of inventory in warehouses or cargo ships in commercial settings and blue force tracking in military scenarios. In cluttered environments where the Global Positioning System (GPS) is often inaccessible (e.g., inside buildings, in urban canyons, under tree canopies, and in caves), multipath, line-of-sight (LoS) blockage, and excess propagation delays through materials present significant challenges to positioning. In such cluttered environments, ultrawide bandwidth (UWB) technology offers potential for achieving high localization accuracy [1–6] due to its ability to resolve multipath and penetrate obstacles [7–12]. The topic of UWB localization was also recently addressed within the framework of the European project PULSERS (Pervasive UWB Low Spectral Energy Radio Systems, http://www.pulsers.eu/). For more information on the fundamentals of UWB, we refer to [13–16], and references therein.

Because the wide transmission bandwidth allows fine delay resolution, several UWB-based localization techniques utilize time-of-arrival (ToA) estimation of the first path to measure the range between a receiver and a transmitter [16–20]. However, the accuracy and reliability of range-only localization techniques typically degenerate in dense cluttered environments, where multipath, (LoS) blockage, and excess propagation delays through materials often lead to positively biased range measurements. A model for this effect is proposed in [21] based on indoor measurements.

To address the problem of localization in indoor environments, we consider a network of fixed beacons (also referred to as anchor nodes) placed in known locations and emitting UWB signals for ranging purposes. The target

(or agent node) estimates the ranges to these beacons, from which it determines its position. The accuracy of range-only localization systems depends mainly on two factors. The first is the geometric configuration of the system, that is, the placement of the beacons relative to the target. The second is the quality of the range measurements themselves [22]. With perfect range measurements to at least three beacons, a target can unambiguously determine its position in two-dimensional space using a triangulation technique. In practice, however, these measurements are corrupted due to the propagation conditions of the environment [4]. Partial and complete LoS blockages lead, for example, to positively biased range estimates. These factors will affect the accuracy of the final position estimate to different degrees. Theoretical bounds for position estimation in the presence of biased range measurements were developed in [6].

The possibility of performing range measurements between any pair of nodes enables the use of cooperation, where targets use range information not only from the beacon nodes but also from each other. It is expected that cooperative positioning achieves better accuracy and coverage than positioning relying solely on the beacons [23, 24]. The natural way to obtain practical cooperative positioning algorithms is to extend existing methods by incorporating range measurements between pairs of target nodes. Unfortunately, the maximum likelihood (ML) approach, though asymptotically efficient (i.e., approaches the Cramér-Rao lower bound for large signal-to-noise ratios), poses several problems (both with and without cooperation) due to the presence of local maxima in the likelihood function and the need for good ranging error statistical models. Several approaches have been proposed in the literature to obtain low-complexity cooperative positioning schemes; a survey can be found in [24]. Among them is a simple linear least square (LS) estimator [25], which transforms the original nonlinear LS problem into a linear one at the expense of some performance loss. A suboptimal hierarchical algorithm for cooperative ML is proposed in [26] and applied to a scenario where range measurements are estimated from received power measurements.

In this paper, a realistic indoor scenario is considered where N beacons are deployed to localize the target(s) using UWB technology. First, we present the results of an extensive measurement campaign, from which models for the ranging error and extra propagation delay caused by the presence of walls were derived. This model is adopted in a two-step positioning algorithm based on the LS technique that improves the positioning accuracy when topology information of the environment is available. We then introduce an iterative version of the LS technique that accounts for cooperation among targets. In the numerical results, the achievable position accuracy is evaluated for different system configurations to show the impact of both the cooperation between agents and the topology configuration. Our results are also compared with the theoretical lower bound obtained using the statistical ranging error model.

The remainder of the paper is organized as follows. In Section 2, we describe the scenario investigated. Section 3 presents the results of the measurement campaign, from which a statistical ranging error model is derived. In Section 4, localization algorithms are presented to estimate the target position. The extension of the algorithms to the cooperative scenario is proposed in Section 5. Finally, numerical results are presented and analyzed in Section 6.

2. THE SCENARIO CONSIDERED

A measurement campaign was performed at the WiLAB, University of Bologna, Italy, to characterize UWB ranging behavior in a typical office indoor environment. The WiLAB building is made of concrete walls 15 and 30 cm thick (see Figure 1). The considered environment is equipped with typical office furniture.

A positioning system composed of $N = 5$ fixed UWB beacons (labeled tx1–5 in Figure 1) was deployed to localize one or more UWB targets. Each ranging device, placed 88 cm above the ground, consisted of one UWB radio operating in the 3.2–7.4 GHz 10 dB RF bandwidth. These commercial radios are equipped to perform ranging by estimating the ToA of the first path using a thresholding technique [20].

A grid of 20 possible target positions (numbered 1–20 in Figure 1) defined the points from which range (distance) measurements were taken at 76 cm height. For each target position, 1500 range measurements were collected from each beacon. In order to test cooperative positioning algorithms, 1500 range measurements were also taken between each possible pair of target locations in the grid. Clearly, a pair of devices can be in non-LoS (NLoS) condition depending on their relative locations within the topology of the environment.

3. MODELING OF THE RANGE MEASUREMENT ERROR

In developing and assessing any localization algorithm, it is important to characterize the ranging error. Understanding the sources and nature of ranging error provides insight into improving positioning performance in difficult environments.

Let us first define a few terms. We refer to a range measurement as a direct path (DP) measurement if it is obtained from a signal traveling along a straight line between the two ranging devices. A measurement is non-DP if the DP signal is completely obstructed and the first signal to arrive at the receiver comes from reflected paths only. A LoS measurement is one obtained when the signal travels along an unobstructed DP, while an NLoS measurement results from either complete or partial DP blockage. In the latter case, the signal has to traverse materials other than air, resulting in excess delay of the DP signal.

Range measurements based on ToA are typically corrupted by four sources: *thermal noise, multipath fading, DP blockage*, and *DP excess delay*. Thermal noise affects the signal-to-noise ratio and thus determines the fundamental error bound on ranging [16]. Multipath fading results from destructive and constructive interference of signals arriving at the receiver via different propagation paths. This interference makes detection of the DP signal, if present, difficult. UWB signals have the distinct advantage of

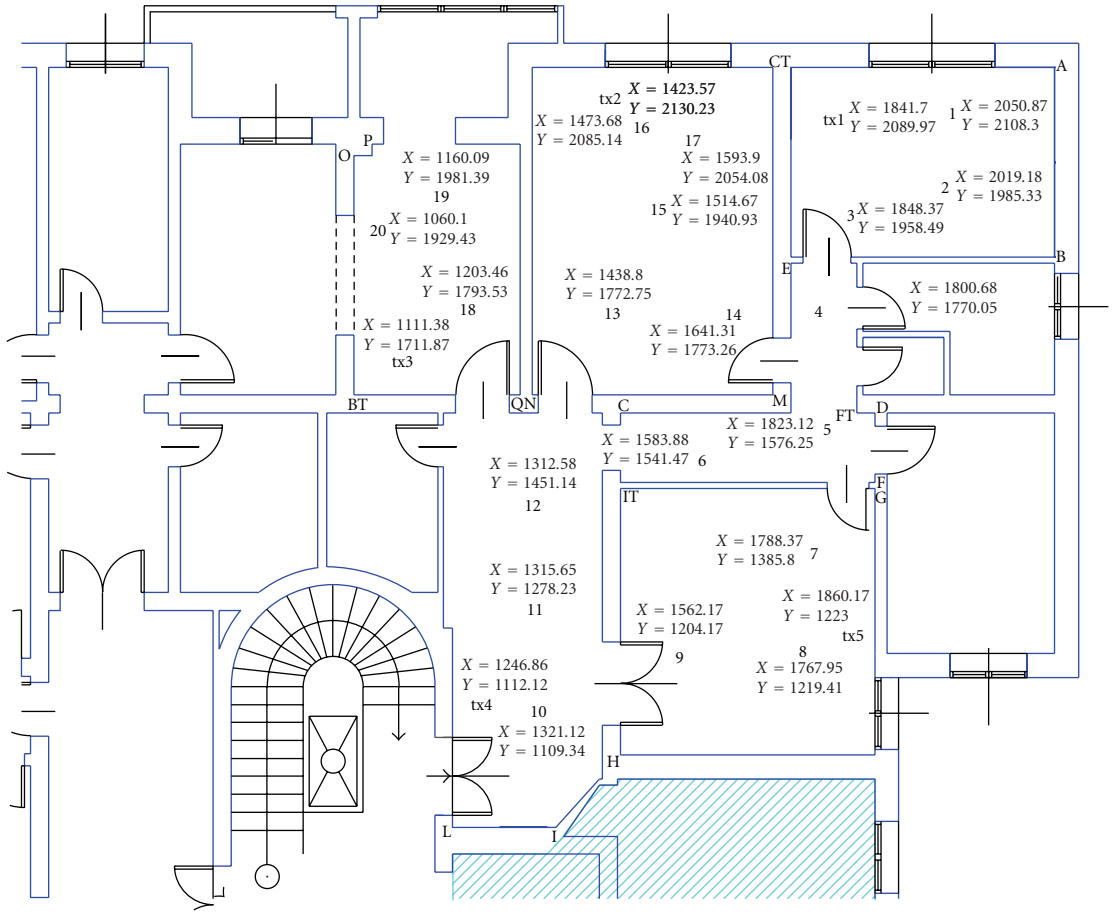

Figure 1: The measurement environment at the WiLAB, University of Bologna, Italy. Coordinates are expressed in centimeters.

resolving multipath components, greatly reducing multipath fading [7–9]. However, the presence of a large number of signal echoes can still make the detection of the first arriving path challenging [20].

The third source of ranging error is *DP blockage*. In some areas of the environment, the DP from certain beacons to the target may be completely obstructed, such that the only received signals are from reflections. The resulting measured ranges are then larger than the true distances. The fourth difficulty is due to *DP excess delay* incurred by propagation of the partially obstructed DP signal through different materials, such as walls. When such a signal is observed as the first arrival, the propagation time depends not only upon the traveled distance, but also upon the encountered materials. Because the propagation of signals is slower in some materials than in the air, the signal arrives with excess delay, yielding again a range estimate larger than the true one. An important observation is that the effects of DP blockage and DP excess delay on the range measurement are the same: they both add a *positive bias* to the true range between ranging devices. We will henceforth refer to such measurements as NLoS. The positive error in NLoS measurements can be a limiting factor in UWB ranging performance and so must be accounted for.

3.1. DP excess delay characterization

As explained above, NLoS ranging measurements are a primary source of localization error. In order to better understand these measurements, we first seek to characterize the positive NLoS bias. A set of ranging measurements was performed to characterize the DP excess delay due to the presence of walls.

Figure 2 depicts the measurement layouts investigated. In the first configuration (Figure 2(a)), a simple concrete wall of thickness $d_W = 15.5$ or $d_W = 30$ cm is present between two ranging devices. In the second configuration (Figure 2(b)), two walls of thicknesses 15 and 30 cm are present. Ranging measurements were collected within 100 cm of the walls to minimize the influence of multipath and better capture the DP excess delay effect. Specifically, ranging measurements were collected for devices located 20, 40, 60, 80, and 100 cm from the surface of the walls. A total of 1500 range measurements were collected for each configuration. Table 1 reports the mean and standard deviation of the ranging error in the collected measurements over all configurations for each layout. As can be noted, the bias due to the excess delay appears to increase linearly with the thickness of the wall. The low value of the standard deviation indicates that the

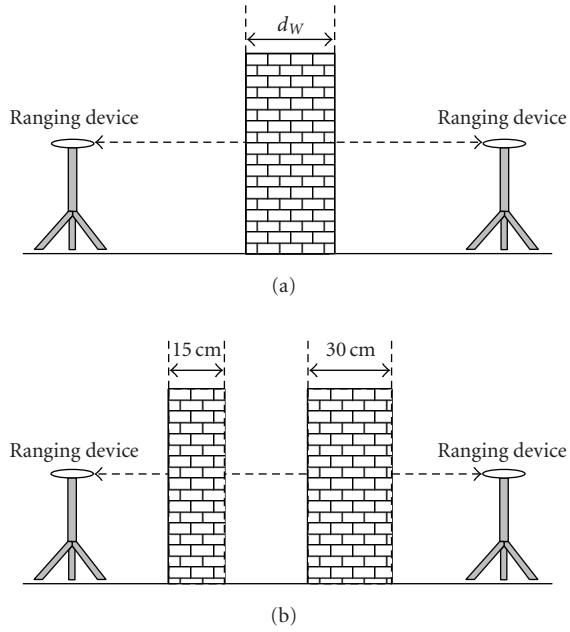

Figure 2: The configurations considered for DP excess delay characterization. (a) 1 wall with thickness $d_W = 15.5$ cm or $d_W = 30$ cm; (b) 2 walls with combined thickness 15.5 + 30 cm.

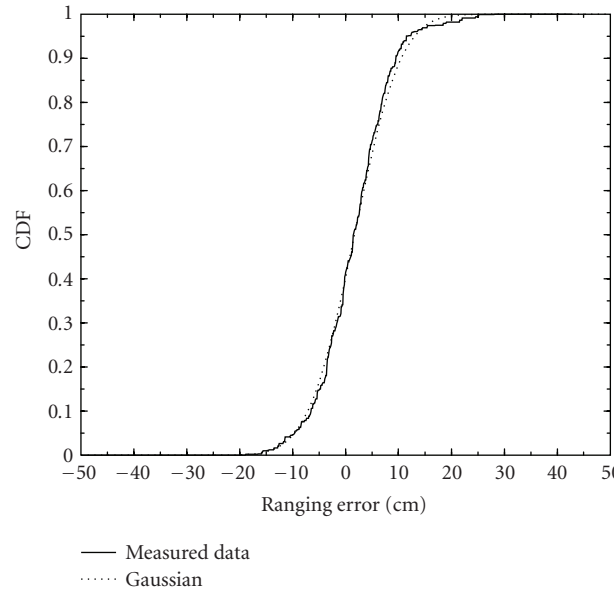

Figure 3: CDF of the ranging error for the LoS condition. Comparison with the Gaussian statistics.

Table 1: Mean and standard deviation of ranging error for different wall thicknesses.

Layout, d_W [cm]	Mean [cm]	std dev [cm]
1 wall, 15.5	16.4	3.7
1 wall, 30	29.5	3.2
2 walls, 15.5 + 30	45.2	3

estimation error is dominated by the effects of DP excess delay rather than multipath or distance-dependent received power.

It is interesting to note that these numerical results can also be considered as an indirect method to estimate the relative electrical permittivity ϵ_r of the material under analysis (in this case, concrete). The speed of the electromagnetic wave travelling inside materials is slowed down by a factor $\sqrt{\epsilon_r}$ with respect to the speed of light, $c \simeq 3 \cdot 10^8$ m/s; hence the theoretical excess delay introduced by a wall of thickness d_W is

$$\Delta = \left(\sqrt{\epsilon_r} - 1\right) \frac{d_W}{c}. \quad (1)$$

We observe in our measurements that $\Delta \simeq d_W/c$, and hence $\epsilon_r \simeq 4$, which is similar to the value obtained in [27].

3.2. Range estimation error

Section 3.1 shows that the excess delay is caused primarily by the number and characteristics of the walls obstructing the DP. We now use the data collected during the main measurement campaign described in Section 2 to derive a simple statistical model for ranging error. The collected ranging measurements were categorized and then analyzed as a function of the number of walls between the ranging devices. The ranging data was then analyzed as a function of the number of walls between the ranging devices. Hence, the data for each condition (LoS, NLoS 1 wall, NLoS 2 walls, etc.) includes measurements taken at varying distances, positions within the environment, wall thicknesses, and other factors.

Table 2 reports the mean and standard deviation of the ranging error for each condition, as well as the frequency of the condition (number of configurations belonging to the condition over the total number of configurations considered). The characterization of the bias for 3,4, and 5 walls is not reported because the number of measurements available was not sufficient to obtain a significant statistic. As can be noted, the bias is strictly related to the number of walls, regardless of the actual distance between the ranging devices.

In Figures 3 and 4, the cumulative distribution functions (CDF) for range measurements collected in the LoS, NLoS 1 wall, and NLoS 2 wall conditions are reported. These CDFs are compared to the Gaussian CDF parameterized by the mean and standard deviation values in Table 2. In all cases, there is a clear match between the measured data and the Gaussian model.

3.3. Statistical model for ranging error

Let $\mathbf{p} = (x, y)^T$ be the vector of the target's coordinates, where the subscript T denotes the transpose. The true distance to the ith beacon of known coordinates (x_i, y_i) is given by

$$d_i = d_i(\mathbf{p}) = \sqrt{(x - x_i)^2 + (y - y_i)^2}, \quad i = 1, \ldots, N. \quad (2)$$

Table 2: Mean, standard deviation, and frequency for ranging error in different wall conditions.

Condition	Mean [cm]	std dev [cm]	Frequency
LoS	1.7	6.9	0.27
NLoS 1 wall	32.4	13.9	0.35
NLoS 2 walls	64.6	23.3	0.28
NLoS 3 walls	N.A.	N.A.	0.05
NLoS 4 walls	N.A.	N.A.	0.03
NLoS 5 walls	N.A.	N.A.	0.02

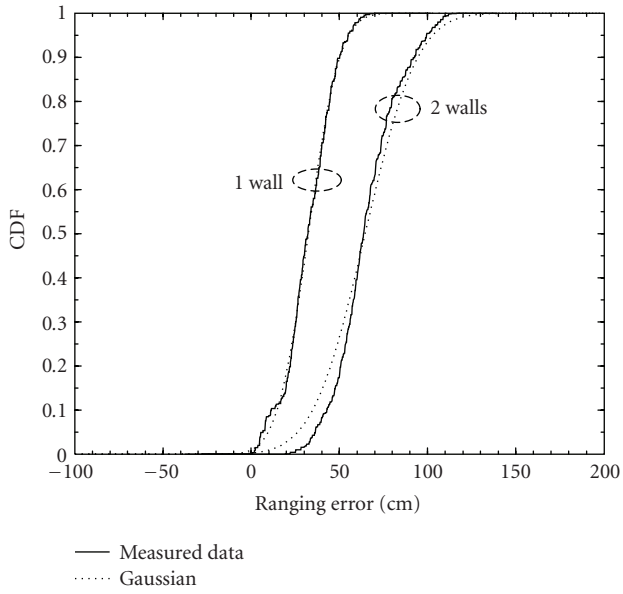

Figure 4: CDF of the ranging error for the NLoS 1-wall and NLoS 2-wall conditions. Comparison with the Gaussian statistics.

We model the range measurement r_i between the target and the ith beacon as

$$r_i = d_i + b_i + \epsilon_i, \tag{3}$$

where b_i is the bias and ϵ_i is Gaussian noise, independent of b_i, with zero mean and variance σ_i^2. The parameter σ_i for the scenario considered can be obtained from Table 2 once the number of walls between the ith beacon and the target node is known.

The probability density function (p.d.f.) of ϵ_i is therefore given by

$$f_{\epsilon_i}(\epsilon) = \frac{1}{\sqrt{2\pi}\sigma_i} e^{-\epsilon^2/2\sigma_i^2}. \tag{4}$$

The bias b_i can be treated either as a random variable, in case a statistical characterization is available, or as a deterministic quantity if it is somehow known. Below, we describe both models of the bias.

3.3.1. Deterministic model for the bias (wall extra delay model)

We have demonstrated that the bias depends primarily on the walls obstructing the DP signal. The bias between the target and the ith beacon, b_i, can therefore be modelled as

$$\begin{aligned} b_i &= E_i \cdot c, \\ E_i &= \sum_{k=1}^{N_e^{(i)}} W_k^{(i)} \cdot \Delta_k, \end{aligned} \tag{5}$$

where E_i is the total time delay caused by NLoS conditions, $W_k^{(i)}$ is the number of walls introducing the same excess delay value Δ_k (e.g., the number of walls of the same material and thickness), and $N_e^{(i)}$ is the number of different excess delay values. The total number of walls separating the ranging devices is $W^{(i)} = \sum_{k=1}^{N_e^{(i)}} W_k^{(i)}$. We name this model the *wall extra delay* (WED) model. When every wall in the scenario has the same thickness and composition (i.e., $\Delta_k = \Delta$ for each k), (5) simplifies to

$$b_i = W^{(i)} \Delta \cdot c. \tag{6}$$

As will be demonstrated in Section 4, a priori knowledge of the bias can sometimes be obtained using the WED model if a preliminary estimate of the target position is available. In that case, the approximate bias value can be simply subtracted from the range measurements. The unbiased distance estimates are then given by

$$\hat{d}_i = r_i - b_i \tag{7}$$

with the following p.d.f., conditioned on the target position $\mathbf{p}$:

$$f_i(\hat{d}_i \mid \mathbf{p}) \equiv f_{\epsilon_i}(\hat{d}_i - d_i). \tag{8}$$

3.3.2. Statistical model for the bias

Alternatively, the bias can be modeled using some priori statistical characterization derived from measurements performed in similar environments. From the results presented earlier in the section, we can conclude that the bias will always be nonnegative. A similar conclusion has been attained by other authors, for example, [28]. The actual value of the bias, however, will depend largely on the environment.

We expect the bias to take a wider range of values in a cluttered environment with many walls, machines, and furniture (such as a typical office building), than in an open space. Note that the bias cannot grow infinitely large, regardless of the propagation environment.

Although a detailed electromagnetic characterization of the environment is rarely available, rough classification of the environment is often feasible, for example, "concrete office building" or "wooden warehouse." By performing range measurements in typical buildings of these classes beforehand, we can assemble a library of histograms to characterize ranging in various environment classes. We can then use these histograms to approximate the probability density function (p.d.f.) of the biases in the particular building of interest.

Let us assume such histograms are available for each beacon. They may differ from beacon to beacon, so we index them by the beacon number i. The ith histogram has $K^{(i)}$ bars, where the kth bar covers the range $\beta_{k-1}^{(i)}$ to $\beta_k^{(i)}$ and has height $p_k^{(i)}$. We can therefore associate the p.d.f. of b_i, $f_{b_i}(b)$, to the histogram according to

$$f_{b_i}(b) \simeq \sum_{k=1}^{K^{(i)}} w_k^{(i)} u_{\{\beta_{k-1}^{(i)}, \beta_k^{(i)}\}}(b), \tag{9}$$

where $w_k^{(i)} = p_k^{(i)}/(\beta_k^{(i)} - \beta_{k-1}^{(i)})$, $u_{\{a,a'\}}(b) = 1$ if $a \le b \le a'$, 0 otherwise, and $\beta_0^{(i)} = 0$. We note that if the DP to beacon i is LoS (i.e., the associated range measurement has no bias), then $f_{b_i}(b) = \delta(b)$, where $\delta(b)$ is the Dirac delta function.

In the absence of an appropriate histogram, the p.d.f. of b_i can be built using topological knowledge of the environment and the WED model (5), with parameters taken from measurements performed in a similar environment class. In this case, $K^{(i)} = N_e^{(i)}$, $\beta_k^{(i)} = \Delta_k \cdot c$, and $p_k^{(i)}$ can be taken as the frequency of all the configurations with the same extra propagation delay Δ_k between the ith beacon and the target. For example, for the scenario considered, $p_k^{(i)}$ equals the frequencies reported in the third column of Table 2.

Even in the absence of any measured data, we can always determine the maximum expected bias β_m for a fixed scenario and, in the absence of other priori information, assume a uniform distribution in $[0, \beta_m]$, that is, $K = 1$, $\beta_1 = \beta_m$, and $w_1 = 1/\beta_m$ [6].

To derive the complete statistical model for range measurements, let us lump the bias term with the Gaussian measurement noise $\tilde{\nu}_i = b_i + \epsilon_i$ and obtain the corresponding p.d.f.

$$\begin{aligned} f_{\tilde{\nu}_i}(\tilde{\nu}_i) &= \int_{-\infty}^{\infty} f_{b_i}(x) f_{\epsilon_i}(\tilde{\nu}_i - x) dx \\ &= \sum_{k=1}^{K^{(i)}} w_k^{(i)} \left[Q\left(\frac{\tilde{\nu}_i - \beta_k^{(i)}}{\sigma_i}\right) - Q\left(\frac{\tilde{\nu}_i - \beta_{k-1}^{(i)}}{\sigma_i}\right) \right], \end{aligned} \tag{10}$$

where $Q(x) = (1/\sqrt{2\pi}) \int_x^{+\infty} e^{-t^2/2} dt$ is the Gaussian Q-function. If the ith beacon is LoS, then ν_i is Gaussian distributed with zero mean and variance σ_i^2. In order to obtain an unbiased estimator, we subtract the mean of $\tilde{\nu}_i$, denoted m_i, from the ith range measurement. This is equivalent to replacing $\tilde{\nu}_i$ by $\nu_i \triangleq \tilde{\nu}_i - m_i$.

The estimated distance is then modeled as

$$\hat{d}_i = d_i + \nu_i, \tag{11}$$

with p.d.f. given by

$$\begin{aligned} f_i(\hat{d}_i \mid \mathbf{p}) = \sum_{k=1}^{K^{(i)}} w_k^{(i)} \Bigg[& Q\left(\frac{\hat{d}_i - d_i + m_i - \beta_k^{(i)}}{\sigma_i}\right) \\ & - Q\left(\frac{\hat{d}_i - d_i + m_i - \beta_{k-1}^{(i)}}{\sigma_i}\right) \Bigg]. \end{aligned} \tag{12}$$

A different approach to modeling the ranging error can be found in [21], where ranging data is analyzed as a function of the true distance instead of the number of walls. However, the Gaussian behavior of the ranging error is also confirmed in that case. Expression (12) can be useful to derive theoretical bounds on positioning; for example, through the approach proposed in [6].

4. LOCALIZATION WITHOUT COOPERATION

The goal of positioning is to determine the locations of the target(s), given a set of measurements (in our case the ranges between nodes). Positioning occurs in two steps. First, ranging measurements are obtained. Then, the measurements are combined using positioning techniques to deduce the location of the target(s). Depending on the availability of a priori knowledge about the environment topology and/or electromagnetic characteristics, different positioning strategies can be adopted.

4.1. Localization without priori information

Multi-lateration is a practical method for determining a node's position. In the presence of ideal range measurements (i.e., $\hat{d}_i = d_i$), the ith beacon defines a circle centered in (x_i, y_i) with radius d_i, upon which the target is located. If the target has obtained ranges to multiple beacons, then the intersection of the circles corresponds to the position of the target node. In a two-dimensional space, at least three beacons are required. Specifically, the position estimate (x, y) is obtained by solving the following system of equations:

$$\begin{aligned} (x_1 - x)^2 + (y_1 - y)^2 &= \hat{d}_1^2, \\ &\vdots \\ (x_N - x)^2 + (y_N - y)^2 &= \hat{d}_N^2. \end{aligned} \tag{13}$$

According to [25], the system of equations in (13) can be linearized by subtracting the last equation from the first $N-1$ equations. The resulting system of linear equations is given by the following matrix form:

$$\mathbf{A} \cdot \mathbf{p} = \mathbf{b}, \tag{14}$$

where

$$\mathbf{A} \triangleq \begin{pmatrix} 2(x_1 - x_N) & 2(y_1 - y_N) \\ \vdots & \vdots \\ 2(x_{N-1} - x_N) & 2(y_{N-1} - y_N) \end{pmatrix},$$
$$\mathbf{b} \triangleq \begin{pmatrix} x_1^2 - x_N^2 + y_1^2 - y_N^2 + \hat{d}_N^2 - \hat{d}_1^2 \\ \vdots \\ x_{N-1}^2 - x_N^2 + y_{N-1}^2 - y_N^2 + \hat{d}_N^2 - \hat{d}_{N-1}^2 \end{pmatrix}. \quad (15)$$

In a realistic scenario where ranging estimation errors are present, (14) may be inconsistent, that is, the circles do not intersect at one point. In that case, the position can be estimated through a standard linear LS approach as

$$\hat{\mathbf{p}} = (\mathbf{A}^T\mathbf{A})^{-1}\mathbf{A}^T\mathbf{b}, \quad (16)$$

with the assumption that $\mathbf{A}^T\mathbf{A}$ is nonsingular and $N \geq 3$ [25]. Particular attention must be paid in selecting the beacon associated with the last equation in (13) and used as reference in (14), (15). If the corresponding range measurement is biased, bias will be introduced in all the equations with a consequent performance loss [29]. This aspect will be investigated in the numerical results.

4.2. Localization with priori information

Our measurement results in Section 3 show that NLoS configurations result in a ranging error bias which is often the major source of positioning error. By analyzing this data, we have also seen that the bias is strictly related to the number of walls encountered by the signal. Assuming that priori knowledge of the environment topology is available, it is possible to refine the target's position estimate once an initial rough estimate has been obtained. In many cases, knowledge of the room in which the target is located will suffice as an initial estimate. These considerations suggest the following two-step positioning algorithm when priori information is available.

(i) *First estimate:* an initial rough position estimate $\hat{\mathbf{p}}^{(1)}$ is obtained using the LS method (16) by setting $\hat{d}_i = r_i$.

(ii) *Range correction:* biases due to propagation through walls are subtracted from range measurements according to (7) and the WED model for b_i in (5), where the number of walls separating the target and each beacon is calculated using the first position estimate and the topology information.

(iii) *Refinement:* a second LS position estimate $\hat{\mathbf{p}}^{(2)}$ is calculated with the corrected (unbiased) range values.

A possible improvement of this two-step algorithm is to identify and select, based on the initial rough position estimate, the reference beacon to be used in (13) during the refinement step of LS position estimate. The reference beacon can be chosen, for example, among those in LoS condition or closer to the target node. In the numerical results the impact of the reference beacon selection will be investigated.

5. LOCALIZATION WITH COOPERATION

Let us now suppose that $U \geq 2$ target nodes are present in the same environment. In the absence of cooperation, each node interacts only with the beacons and estimates its position using, for example, the LS approach (16). It is expected that if the targets are able to make range measurements not only from the beacons but also from each other, thus cooperating, then they can potentially improve their position estimation accuracy.

We define $M = N + U$ as the total number of radio devices (beacons plus targets) present in the system and $r_{i,m}$ for $i, m = 1, 2, \ldots, M$ as the range measurements between the ith and the mth devices. We do not consider ranges measured between beacons. To make use of the range measurements among target nodes, the following *iterative LS algorithm* is proposed.

(1) Set $n = 1$. Using (16) (or the two-step algorithm described in Section 4.2), determine the position estimates $\hat{\mathbf{p}}_j^{(1)}$ for the targets, that is, $j = 1, 2, \ldots, U$, by setting $\hat{d}_i = r_{i,j+N}$ with $i = 1, 2, \ldots, N$.

(2) Set $n = n + 1$. For each target $j = 1, 2, \ldots, U$, the LS algorithm is applied by treating the other $U - 1$ targets as additional "virtual" beacons located at the estimated positions $\hat{\mathbf{p}}_j^{(n)}$ obtained during the previous step. Specifically, the matrices $\mathbf{A}^{(n,j)}$ and $\mathbf{b}^{(n,j)}$ at step n and for the jth target are now

$$\mathbf{A}^{(n,j)} \triangleq \begin{pmatrix} 2(x_1 - x_N) & 2(y_1 - y_N) \\ \vdots & \vdots \\ 2(x_{N-1} - x_N) & 2(y_{N-1} - y_N) \\ 2(\hat{x}_{N+1} - x_N) & 2(\hat{y}_{N+1} - y_N) \\ \vdots & \vdots \\ 2(\hat{x}_{N+j-1} - x_N) & 2(\hat{y}_{N+j-1} - y_N) \\ 2(\hat{x}_{N+j+1} - x_N) & 2(\hat{y}_{N+j+1} - y_N) \\ \vdots & \vdots \\ 2(\hat{x}_M - x_N) & 2(\hat{y}_M - y_N) \end{pmatrix},$$
$$\mathbf{b}^{(n,j)} \triangleq \begin{pmatrix} x_1^2 - x_N^2 + y_1^2 - y_N^2 + \hat{d}_N^2 - \hat{d}_1^2 \\ \vdots \\ x_{N-1}^2 - x_N^2 + y_{N-1}^2 - y_N^2 + \hat{d}_N^2 - \hat{d}_{N-1}^2 \\ \hat{x}_{N+1}^2 - x_N^2 + \hat{y}_{N+1}^2 - y_N^2 + \hat{d}_N^2 - \hat{d}_{N+1}^2 \\ \vdots \\ \hat{x}_{N+j-1}^2 - x_N^2 + \hat{y}_{N+j-1}^2 - y_N^2 + \hat{d}_N^2 - \hat{d}_{N+j-1}^2 \\ \hat{x}_{N+j+1}^2 - x_N^2 + \hat{y}_{N+j+1}^2 - y_N^2 + \hat{d}_N^2 - \hat{d}_{N+j+1}^2 \\ \vdots \\ \hat{x}_M^2 - x_N^2 + \hat{y}_M^2 - y_N^2 + \hat{d}_N^2 - \hat{d}_M^2 \end{pmatrix}, \quad (17)$$

by setting $\hat{d}_i = r_{i,j+N}$ for $i = 1, 2, \ldots, M$. The LS position estimate for the jth target at step n is therefore

$$\hat{\mathbf{p}}_j^{(n)} = \left(\mathbf{A}^{(n,j)^T}\mathbf{A}^{(n,j)}\right)^{-1}\mathbf{A}^{(n,j)^T}\mathbf{b}^{(n,j)}. \quad (18)$$

(3) If $n \geq N_{\text{iter}}$ stop; else go to (2).

The algorithm stops when a predefined number N_{iter} of iterations is reached. Again, the reference beacon in (17) can be selected when the reliability of range measurement is known.

6. NUMERICAL RESULTS

In this section, we present a localization performance based on experimental data. First, a scenario with only one target (i.e., in the absence of cooperation) is considered.

Figure 5 shows the root mean square error (RMSE) of the estimation for each location in the grid (identified by the node ID) is reported for the case of $N = 3$ (tx1,tx3,tx5) and $N = 5$ beacons. There is no priori information about the environment topology, and beacon tx5 is chosen as the reference node. It can be seen that for all locations the use of a larger number of beacons does not necessarily correspond to better positioning accuracy. This is due to the fact that, in many cases, the added range measurements and/or the chosen reference node are subject to large errors, which cannot be corrected due to the absence of a priori information. Moreover, the geometric configuration of the additional beacons may not improve the positioning accuracy in certain locations.

Next, we examine the effect of a priori information and excess delay correction on positioning. The RMSE for localization attained by the two-step algorithm presented in Section 4.2 is reported in Figure 6. It can be seen that positioning errors less than 1 meter are achieved in most locations. By comparing Figures 5 and 6, we can conclude that the correction of the range measurements using the WED model and knowledge of the environment topology leads to a significant performance improvement for many locations.

We mentioned in Section 4.2 that the wrong choice of the reference beacon in the linear LS approach may lead to significant performance degradation. This aspect is investigated in Figure 7, where the best reference for each target location is chosen from the set of 5 beacons, in order to obtain the lowest RMSE with or without bias compensation. By comparing Figure 7 with Figures 5 and 6, we observe that the selection of the right reference beacon can further improve the positioning accuracy in both cases.

The effect of cooperation on localization is investigated in Figures 8, 9, and 10. Figure 8 presents the RMSE as a function of the number of iterations N_{iter} of the iterative LS algorithm proposed in Section 5. We assume $N = 3$ beacons (tx1,tx3,tx5) and two targets with the capability to perform intertarget range measurements. Target 1 is located in position 8, and the cooperating node (target 2) is located in position 10 (LoS condition) or 18 (NLoS condition). Beacon tx5 is assumed as reference for the LS algorithm. These configurations were chosen because they lead to two

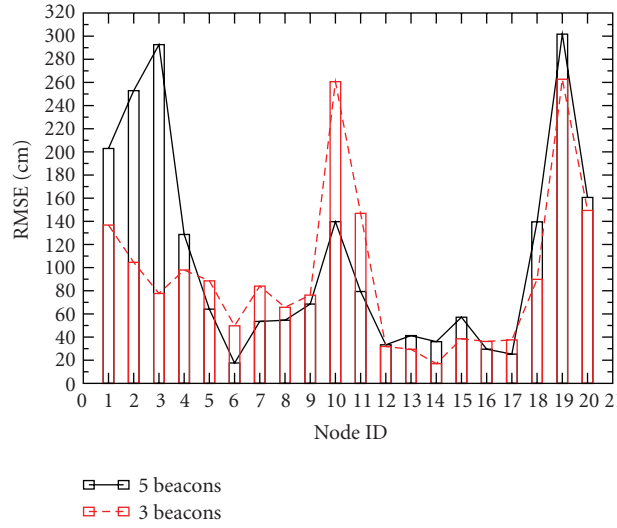

Figure 5: RMSE as a function of target position in the absence of priori information. $N = 3$ (tx1,tx3,tx5) and $N = 5$ beacons are considered.

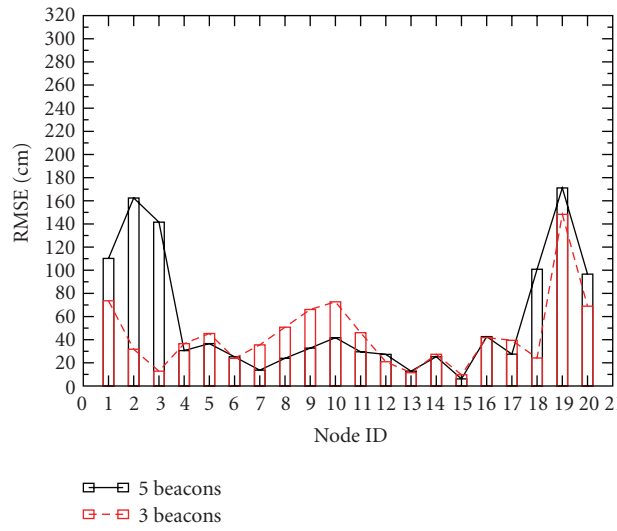

Figure 6: RMSE as a function of target position in the presence of priori information (two-step algorithm). $N = 3$ (tx1,tx3,tx5) and $N = 5$.

distinct interesting situations. When the two targets are located in LoS, they can perform a highly accurate intertarget range measurements. When the targets are located in NLoS (different rooms), the intertarget range measurements are expected to be worse. Figure 8 shows that cooperation in LoS can strongly improve the RMSE and that the iterative LS algorithm converges after few iterations. Note also that the resulting RMSE for cooperation with 2 iterations and $N = 3$ beacons is better than the case of $N = 5$ beacons without cooperation (Figure 6). In Figure 9, the same situation is considered, but the iterative LS algorithm takes the cooperative node (target 2) as reference instead of beacon tx5. Note that when the reference node is given by a cooperative node in NLoS conditions with respect to the

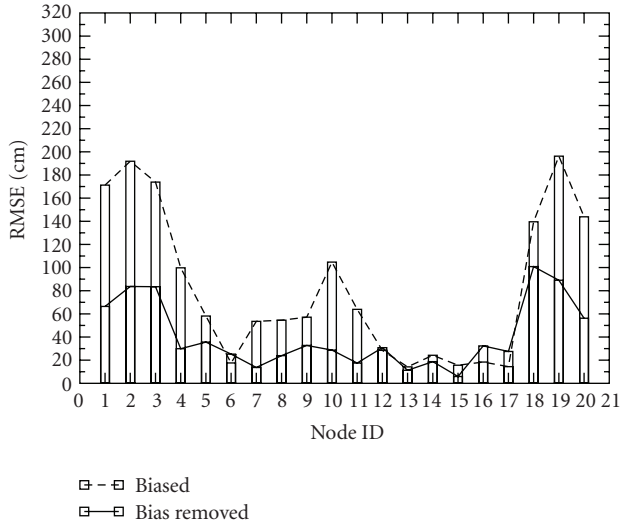

Figure 7: RMSE as a function of target position in the absence and presence of priori information (i.e., with the bias and after removing the bias), using the best selection for reference beacon. $N = 5$ beacons are considered.

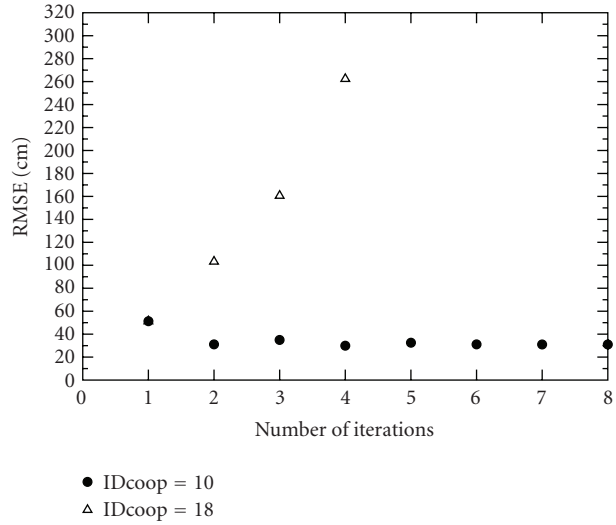

Figure 9: RMSE as a function of number of iterations when target 1, located in position 8, cooperates with target 2, in position 10 or 18. $N = 3$ (tx1,tx3,tx5) beacons are considered. The cooperative node is taken as reference for the LS algorithm.

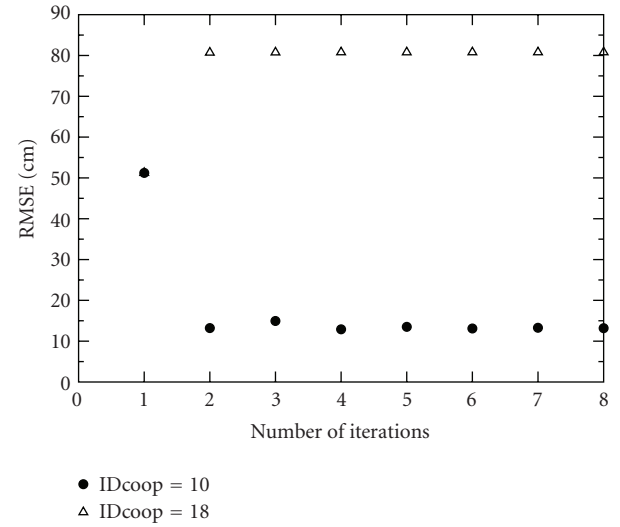

Figure 8: RMSE as a function of number of iterations when target 1, located in position 8, cooperates with target 2, in position 10 or 18. $N = 3$ (tx1,tx3,tx5) beacons are considered. Tx5 is taken as reference for the LS algorithm.

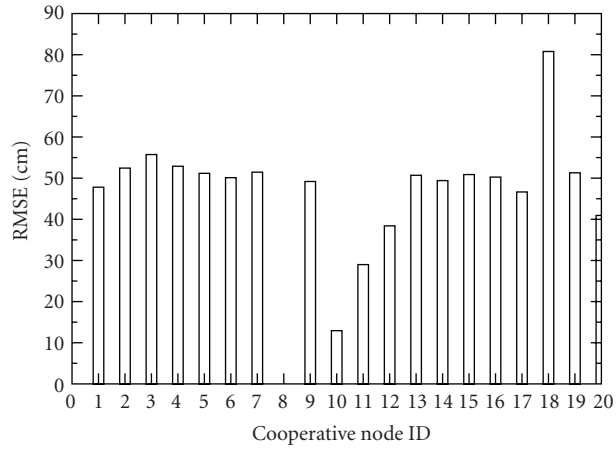

Figure 10: RMSE as a function of target 2 position when target 1, located in position 8, cooperates with target 2; $N = 3$ (tx1,tx3,tx5) beacons are considered, $N_{\text{iter}} = 4$.

target, for example, when target 2 is in position 10, the RMSE increases with each iteration. Meanwhile, when target 2 is in LoS, position 18, the RMSE remains roughly the same after the second iteration. In Figures 9 and 10, we can also compare the RMSE before the targets cooperate (iteration 1) to the RMSE after cooperation (iterations 2 and up). In both cases, cooperation reduces the localization error when the target nodes are in LoS.

Finally, in Figure 10 we examine localization performance as a function of the position of the cooperating node. We consider the case of $N = 3$ beacons (tx1, tx3, tx5) and $N_{\text{iter}} = 4$ iterations when target 1, located in position 8, cooperates with target 2, whose position varies. As can be noted, the effect of cooperation varies with the position of the cooperating node. In our scenario, the position of target 2 yielding the best performance is 10, in which the cooperating node is in LoS. However, LoS positions 7 and 9 do not lead to any performance gain. Moreover, positions 11 and 12 give significant improvement over the noncooperating algorithm, despite the fact that the cooperating node is in NLoS. Clearly, the intertarget link reliability and the geometric configuration of the nodes both have significant impacts in determining the localization error accuracy.

7. CONCLUSIONS

In this paper, the range estimation error between UWB devices was characterized using measured data in a typical indoor environment. These measurements showed that the extra propagation delay is due primarily to the presence of walls. A deterministic model (WED) for the extra propagation delay and a statistical model for the range estimation error were proposed. A two-step LS positioning algorithm incorporating the WED model was introduced to correct the range measurements in NLoS conditions when the layout of the environment is known. Results showed that a significant gain in localization accuracy can be obtained by the two-step algorithm and that an increase in the number of nodes does not always result in performance gain, depending on the geometric configuration of the nodes. In addition, the choice of the reference node in the LS approach is an important aspect that can have a significant impact on localization accuracy.

An iterative LS algorithm was proposed to exploit cooperation among targets. Results revealed that cooperation is not always advantageous. In fact, it was shown that the geometric configuration of the devices may have a stronger impact than the quality of the intertarget range estimates on the localization accuracy. This is an important consideration when deriving guidelines for cooperation in positioning algorithms.

ACKNOWLEDGMENTS

The authors would like to thank M. Chiani and H. Wymeersch for helpful discussions. We also thank P. Pinto, A. Giorgetti, N. Decarli, T. Pavani, R. Soloperto, L. Zuari, and R. Conti for their cooperation during measurement data collection and postprocessing. Finally, we would like to thank O. Andrisano for motivating this work and for hosting the measurement campaign at WiLAB. This work has been performed in part within the framework of FP7 European Project EUWB (Grant no. 215669), the National Science Foundation (Grant ECS-0636519) and Jet Propulsion Laboratory-Strategic University Research Partnership Program.

REFERENCES

[1] R. J. Fontana and S. J. Gunderson, "Ultra-wideband precision asset location system," in *Proceedings of the IEEE Conference on Ultra Wideband Systems and Technologies (UWBST '02)*, pp. 147–150, Baltimore, Md, USA, May 2002.

[2] L. Stoica, S. Tiuraniemi, A. Rabbachin, and I. Oppermann, "An ultra wideband TAG circuit transceiver architecture," in *Proceedings of the International Workshop on Ultra Wideband Systems. Joint with Conference on Ultrawideband Systems and Technologies (UWBST & IWUWBS '04)*, pp. 258–262, Kyoto, Japan, May 2004.

[3] D. Dardari, "Pseudo-random active UWB reflectors for accurate ranging," *IEEE Communications Letters*, vol. 8, no. 10, pp. 608–610, 2004.

[4] S. Gezici, Z. Tian, G. B. Giannakis, et al., "Localization via ultra-wideband radios: a look at positioning aspects of future sensor networks," *IEEE Signal Processing Magazine*, vol. 22, no. 4, pp. 70–84, 2005.

[5] Y. Qi, H. Kobayashi, and H. Suda, "Analysis of wireless geolocation in a non-line-of-sight environment," *IEEE Transactions on Wireless Communications*, vol. 5, no. 3, pp. 672–681, 2006.

[6] D. Jourdan, D. Dardari, and M. Z. Win, "Position error bound for UWB localization in dense cluttered environments," *IEEE Transactions on Aerospace and Electronic Systems*, vol. 44, no. 2, pp. 613–628, 2008.

[7] M. Z. Win and R. A. Scholtz, "On the robustness of ultra-wide bandwidth signals in dense multipath environments," *IEEE Communications Letters*, vol. 2, no. 2, pp. 51–53, 1998.

[8] M. Z. Win and R. A. Scholtz, "On the energy capture of ultra -wide bandwidth signals in dense multipath environments," *IEEE Communications Letters*, vol. 2, no. 9, pp. 245–247, 1998.

[9] M. Z. Win and R. A. Scholtz, "Characterization of ultra-wide bandwidth wireless indoor channels: a communication-theoretic view," *IEEE Journal on Selected Areas in Communications*, vol. 20, no. 9, pp. 1613–1627, 2002.

[10] C.-C. Chong and S. K. Yong, "A generic statistical-based UWB channel model for high-rise apartments," *IEEE Transactions on Antennas and Propagation*, vol. 53, no. 8, pp. 2389–2399, 2005.

[11] D. Cassioli, M. Z. Win, and A. F. Molisch, "The ultra-wide bandwidth indoor channel: from statistical model to simulations," *IEEE Journal on Selected Areas in Communications*, vol. 20, no. 6, pp. 1247–1257, 2002.

[12] A. F. Molisch, D. Cassioli, C.-C. Chong, et al., "A comprehensive standardized model for ultrawideband propagation channels," *IEEE Transactions on Antennas and Propagation*, vol. 54, no. 11, part 1, pp. 3151–3166, 2006.

[13] M. Z. Win and R. A. Scholtz, "Impulse radio: how it works," *IEEE Communications Letters*, vol. 2, no. 2, pp. 36–38, 1998.

[14] M. Z. Win and R. A. Scholtz, "Ultra-wide bandwidth time-hopping spread-spectrum impulse radio for wireless multiple-access communications," *IEEE Transactions on Communications*, vol. 48, no. 4, pp. 679–689, 2000.

[15] W. Suwansantisuk and M. Z. Win, "Multipath aided rapid acquisition: optimal search strategies," *IEEE Transactions on Information Theory*, vol. 53, no. 1, pp. 174–193, 2007.

[16] D. Dardari, C.-C. Chong, and M. Z. Win, "Improved lower bounds on time-of-arrival estimation error in realistic UWB channels," in *Proceedings of the IEEE International Conference on Ultra-Wideband (ICUWB '06)*, pp. 531–537, Waltham, Mass, USA, September 2006.

[17] D. Dardari and M. Z. Win, "Threshold-based time-of-arrival estimators in UWB dense multipath channels," in *Proceedings of the IEEE International Conference on Communications (ICC '06)*, vol. 10, pp. 4723–4728, Istanbul, Turkey, June 2006, Also in *IEEE Transactions on Communications*, August 2008.

[18] C. Falsi, D. Dardari, L. Mucchi, and M. Z. Win, "Time of arrival estimation for UWB localizers in realistic environments," *Eurasip Journal on Applied Signal Processing*, vol. 2006, Article ID 32082, p. 13, 2006.

[19] K. Yu and I. Oppermann, "Performance of UWB position estimation based on time-of-arrival measurements," in *Proceedings of the International Workshop on Ultra Wideband Systems. Joint with Conference on Ultrawideband Systems and Technologies (UWBST & IWUWBS '04)*, pp. 400–404, Kyoto, Japan, May 2004.

[20] D. Dardari, A. Conti, U. Ferner, A. Giorgetti, and M. Z. Win, "Ranging with ultrawide bandwidth signals in multipath environments," to appear in *Proceedings of the IEEE*, Special Issue on UWB Technology & Emerging Applications, 2008.

[21] B. Alavi and K. Pahlavan, "Modeling of the TOA-based distance measurement error using UWB indoor radio measurements," *IEEE Communications Letters*, vol. 10, no. 4, pp. 275–277, 2006.

[22] D. Jourdan, D. Dardari, and M. Z. Win, "Position error bound for UWB localization in dense cluttered environments," in *Proceedings of the IEEE International Conference on Communications (ICC '06)*, vol. 8, pp. 3705–3710, Istanbul, Turkey, June 2006.

[23] E. G. Larsson, "Cramér-Rao bound analysis of distributed positioning in sensor netwroks," *IEEE Signal Processing Letters*, vol. 11, no. 3, pp. 334–337, 2004.

[24] N. Patwari, J. N. Ash, S. Kyperountas, A. O. Hero III, R. L. Moses, and N. S. Correal, "Locating the nodes: cooperative localization in wireless sensor networks," *IEEE Signal Processing Magazine*, vol. 22, no. 4, pp. 54–69, 2005.

[25] J. J. Caffery Jr., "A new approach to the geometry of TOA location," in *Proceedings of the 52nd IEEE Vehicular Technology Conference (VTC '00)*, vol. 4, pp. 1943–1949, Boston, Mass, USA, September 2000.

[26] D. Dardari and A. Conti, "A sub-optimal hierarchical maximum likelihood algorithm for collaborative localization in ad-hoc network," in *Proceedings of the 1st Annual IEEE Communications Society Conference on Sensor and Ad Hoc Communications and Networks (SECON '04)*, pp. 425–429, Santa Clara, Calif, USA, October 2004.

[27] A. Muqaibel, A. Safaai-Jazi, A. Bayram, A. M. Attiya, and S. M. Riad, "Ultrawideband through-the-wall propagation," *IEE Proceedings—Microwaves, Antennas and Propagation*, vol. 152, no. 6, pp. 581–588, 2005.

[28] D. B. Jourdan, J. J. Deyst Jr., M. Z. Win, and N. Roy, "Monte Carlo localization in dense multipath environments using UWB ranging," in *Proceedings of the IEEE International Conference on Ultra-Wideband (ICU '05)*, pp. 314–319, Zurich, Switzerland, September 2005.

[29] I. Guvenc, C.-C. Chong, and F. Watanabe, "Analysis of a linear least-squares localization technique in LOS and NLOS environments," in *Proceedings of the 65th IEEE Vehicular Technology Conference (VTC '07)*, pp. 1886–1890, Dublin, Ireland, April 2007.